

Detection and Evaluation of Renal Injury in Burst Wave Lithotripsy Using Ultrasound and Magnetic Resonance Imaging

Philip C. May, MD,^{1,2} Wayne Kreider, PhD,¹ Adam D. Maxwell, PhD,² Yak-Nam Wang, PhD,¹
Bryan W. Cunitz, MS,¹ Philip M. Blomgren, BLA,³ Cynthia D. Johnson, MS,³ Joshua S.H. Park, BA,⁴
Michael R. Bailey, PhD,^{1,2} Donghoon Lee, PhD,⁴ Jonathan D. Harper, MD,² and Mathew D. Sorensen, MD, MS^{2,5}

Abstract

Purpose: Burst wave lithotripsy (BWL) is a transcutaneous technique with potential to safely and effectively fragment renal stones. Preclinical investigations of BWL require the assessment of potential renal injury. This study evaluates the capabilities of real-time ultrasound and MRI to detect and evaluate BWL injury that was induced in porcine kidneys.

Materials and Methods: Ten kidneys from five female farm pigs were treated with either a 170 or 335 kHz BWL transducer using variable treatment parameters and monitored in real-time with ultrasound. Eight kidneys were perfusion fixed and scanned with a 3-Tesla MRI scanner (T1-weighted, T2-weighted, and susceptibility-weighted imaging), followed by processing via an established histomorphometric technique for injury quantification. In addition, two kidneys were separately evaluated for histologic characterization of injury quality.

Results: Observed B-mode hyperechoes on ultrasound consistent with cavitation predicted the presence of BWL-induced renal injury with a sensitivity and specificity of 100% in comparison to the histomorphometric technique. Similarly, MRI detected renal injury with a sensitivity of 90% and specificity of 100% and was able to identify the scale of lesion volumes. The injuries purposefully generated with BWL were histologically similar to those formed by shock wave lithotripsy.

Conclusions: BWL-induced renal injury can be detected with a high degree of sensitivity and specificity by real-time ultrasound and post-treatment *ex vivo* MRI. No injury occurred in this study without cavitation detected on ultrasound. Such capabilities for injury detection and lesion volume quantification on MRI can be used for preclinical testing of BWL.

Keywords: extracorporeal shock wave lithotripsy, renal injury, burst wave lithotripsy, nephrolithiasis

Introduction

BURST WAVE LITHOTRIPSY (BWL) is a method for transcutaneously fragmenting renal stones under investigation at the University of Washington.¹ BWL uses short, broadly focused bursts of ultrasound (US) at lower pressure amplitudes than extracorporeal shock wave lithotripsy (SWL) to fragment stones. *In vitro* studies of BWL demonstrated efficacy at fragmenting natural and artificial calculi.¹ Fragment size was found to be predictable and was regulated by altering the US frequency. Due to the low-pressure

amplitudes and the ability to control fragment size, BWL has significant potential advantages over SWL in the management of renal stones. Demonstrating safety with exposure to renal parenchyma is a critical step in the development of this technology for clinical use.

The purpose of this study was to develop imaging techniques for assessing BWL-induced renal injury in a porcine model. Tissues were treated at a variety of treatment parameters with therapeutic efficacy, including parameters intended to elicit renal parenchymal injury. We assessed the ability of real-time US imaging to detect injury during BWL

¹University of Washington Applied Physics Lab, Center for Industrial and Medical Ultrasound, Seattle, Washington.

²Department of Urology, University of Washington School of Medicine, Seattle, Washington.

³Department of Anatomy and Cell Biology, Indiana University, Indianapolis, Indiana.

⁴Department of Radiology, University of Washington, Seattle, Washington.

⁵Division of Urology, Department of Veteran Affairs Medical Center, Seattle, Washington.

treatments. In addition, we employed an established histomorphometric technique developed to quantify hemorrhagic renal injury in SWL and used it to determine the ability of MRI to detect and quantify injury.²

Materials and Methods

Animal model

All protocols and procedures were approved by the University of Washington's Institutional Animal Care and Use Committee. Five female pigs weighing 55 to 60 kg each were used to assess renal injury from BWL. The pig model has similar size and renal anatomy to humans, and has been used in research for evaluation of injury caused by SWL.² Each animal received general anesthesia induced with 4 mg/kg telazol and maintained with isoflurane. Cardiopulmonary function was monitored. Due to geometric constraints of available BWL transducers as well as a desire to deliver repeatable, known pressures to targeted sites, intra-abdominal treatments were performed. Animals were placed supine and a mid-line incision was made to gain access to the kidneys. The abdominal cavity was filled with degassed phosphate-buffered saline solution before coupling the BWL treatment probe directly to the anterior surface of the exposed renal capsule for treatment. The animals were euthanized following treatment; the eight kidneys were perfusion fixed with 2.5% glutaraldehyde in 0.1 M sodium cacodylate buffer for MRI and histomorphometric analysis. Two kidneys were prepared for histological characterization of injury using hematoxylin and eosin (H&E) staining.

BWL exposure and US imaging

BWL treatment was administered with a custom, low frequency transducer (170 or 335 kHz) to produce a broadly focused US beam with dimensions comparable to those used in SWL. Each transducer had a coupling cone filled with degassed water with an acoustic window made from a silicone rubber membrane, which was gently pressed against the kidney capsule. An in-line US imaging probe (P7-4 or P4-2; Philips Healthcare, Bothell, WA) and a research US imager (V-1; Verasonics, Kirkland, WA) were used to align the BWL transducer focus with the targeted position in the kidney. Real-time B-mode US images were monitored to detect cavitation within the renal parenchyma. Cavitation was identified visually as an area of dynamic hyperechoic activity within the kidney parenchyma or collecting space that appeared during exposure (Supplementary Movie S1; Supplementary Data are available online at www.liebertpub.com/end).³

Each kidney was treated in three sites: upper, middle, and lower poles, which were identified using US visualization of the renal pelvis as a landmark. BWL exposures up to 30 minutes were delivered using bursts with amplitudes from 5.8 to 8.1 MPa with a pulse length of 10 cycles at 170 kHz or 20 cycles at 335 kHz. A burst repetition rate of 40 Hz was used for all treatments at 335 kHz; for several treatments at 170 kHz, a burst repetition rate of 200 Hz was used. Treatments were monitored using B-mode US. Cavitation was expected to cause renal injury, so the exposure durations with cavitation detected by US were varied to permit assessment of injury evolution.

Magnetic resonance imaging

All kidneys were perfusion fixed *in situ* before being surgically removed for *ex vivo* MRI. T1-weighted (recycle delay time [TR]/echo time [TE]=633/23 ms), T2-weighted (TR/TE=7990/75 ms), and susceptibility-weighted (TR/TE=14.7/20.8 ms) imaging was performed using a 3-Tesla MRI scanner (Achieva; Philips Healthcare, Best, The Netherlands). T1-weighted and T2-weighted turbo spin echo sequences were compared to correlate injured regions. A gradient echo-based sequence was used for susceptibility-weighted imaging to identify micro-hemorrhagic areas. Gradient echo T1-weighted (TE/TE=178/2.4 ms, flip angle=3°) imaging was conducted to identify injured regions and to examine sample positions. T1-weighted and T2-weighted imaging sequences were performed with 156 μm in-plane resolution and 1 mm slice thickness; susceptibility-weighted imaging was performed with 450 μm in-plane resolution and 2 mm slice thickness.

Each MRI was evaluated by three reviewers, blinded to the BWL treatment parameters. A site was considered injured if two or more reviewers agreed. Injured regions were best visualized with T2-weighted images, which were used to calculate hemorrhagic injury volume. Susceptibility-weighted and T1-weighted images were used to help confirm the presence or absence of a lesion. Functional renal volume was reconstructed in software (Amira 3D; FEI, Hillsboro, OR) by manually identifying the renal parenchyma and excluding sinus structures on each slice of the T2-weighted images. Hemorrhagic injury was calculated as a percentage of functional renal volume where injury involved the parenchyma, and a total renal volume when hemorrhage included sinus structures. Sensitivity and specificity were determined by comparison to histomorphometric assessment as the gold standard for identifying renal injury.

Histomorphometric tissue analysis

The volume resolution using histomorphometric analysis is 0.1% of functional renal volume. Following MRI, kidneys were sent to Indiana University School of Medicine for histomorphometric analysis.² In brief, following perfusion fixation and MRI scanning, the renal vasculature was cast with yellow Microfil (Flow Tech, Inc., Carver, MA). The kidneys were dehydrated in serial ethanol (30, 100%) and chloroform (100%) solutions. Each kidney was then infiltrated with paraffin (Shandon Hypercenter XP; Thermo Fisher Scientific, Waltham, MA) and serially sectioned with 40 μm slice thickness using a sliding microtome (American Optical No. 860). A digital image of the sectioned surface of the kidney was obtained every 120 μm . Renal sinus regions were manually marked on each image slice to enable subtraction from the total renal area to calculate functional volume of the renal parenchyma. Hemorrhagic lesions were identified on digital images and quantified by pixel color (Adobe Photoshop CS6, 13.0.6; Adobe Systems, Inc., San Jose, CA).

Histologic characterization of renal lesions

Two perfusion fixed kidneys were grossly cut into thirds to analyze each treatment site, and axial segments were processed for histological analysis. Five-micron sections were taken every 1 mm and stained with H&E. Sections were imaged in an upright microscope and evaluated for evidence of hemorrhage and mechanical disruption to determine the nature of the injury.

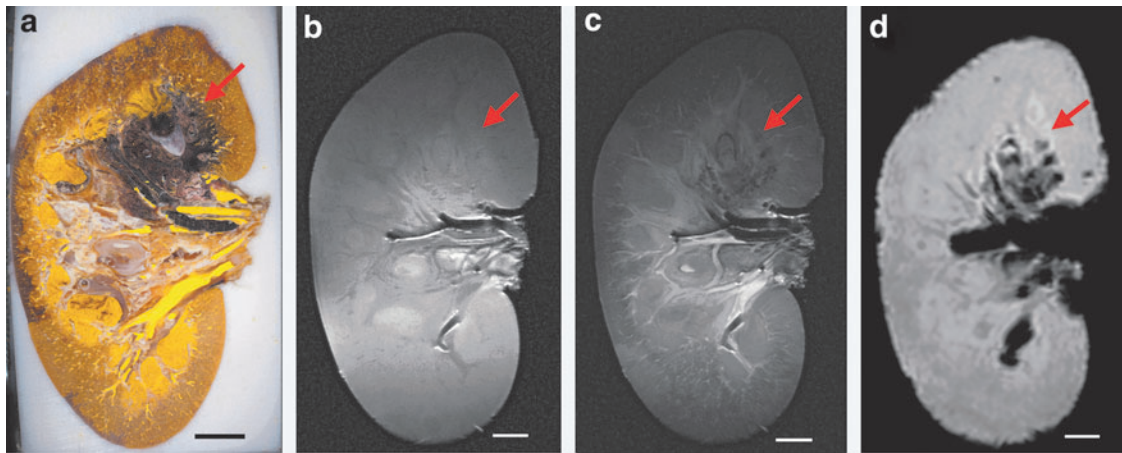


FIG. 1. A comparison of injury visualization for the same kidney specimen in a histomorphometric image (a), and in images using three different MRI sequences: T1-weighted (b), T2-weighted (c), and susceptibility-weighted (d). Images were obtained from Kidney 2, with injury site 2-M (Fig. 3 and Table 1) denoted by a red arrow. Scale bars represent 1 cm.

Results

Detection of injury

Cavitation was observed in real-time on B-mode US as an area of dynamic hyperechogenicity (Supplementary Movie S1) that occurred suddenly in the collecting space and kidney parenchyma during the treatment. Cavitation often did not appear

until several seconds or even minutes into treatment. This detection was then compared to histomorphometric and MRI analyses obtained from fixed kidneys (Fig. 1). As indicated in Figure 1, hemorrhagic injury appears as dark purple/black in histomorphometric images (Fig. 1a). From MRI, injured regions appear hypointense on T2-weighted and susceptibility-weighted images (Fig. 1c, d); although injury sites were detectable on

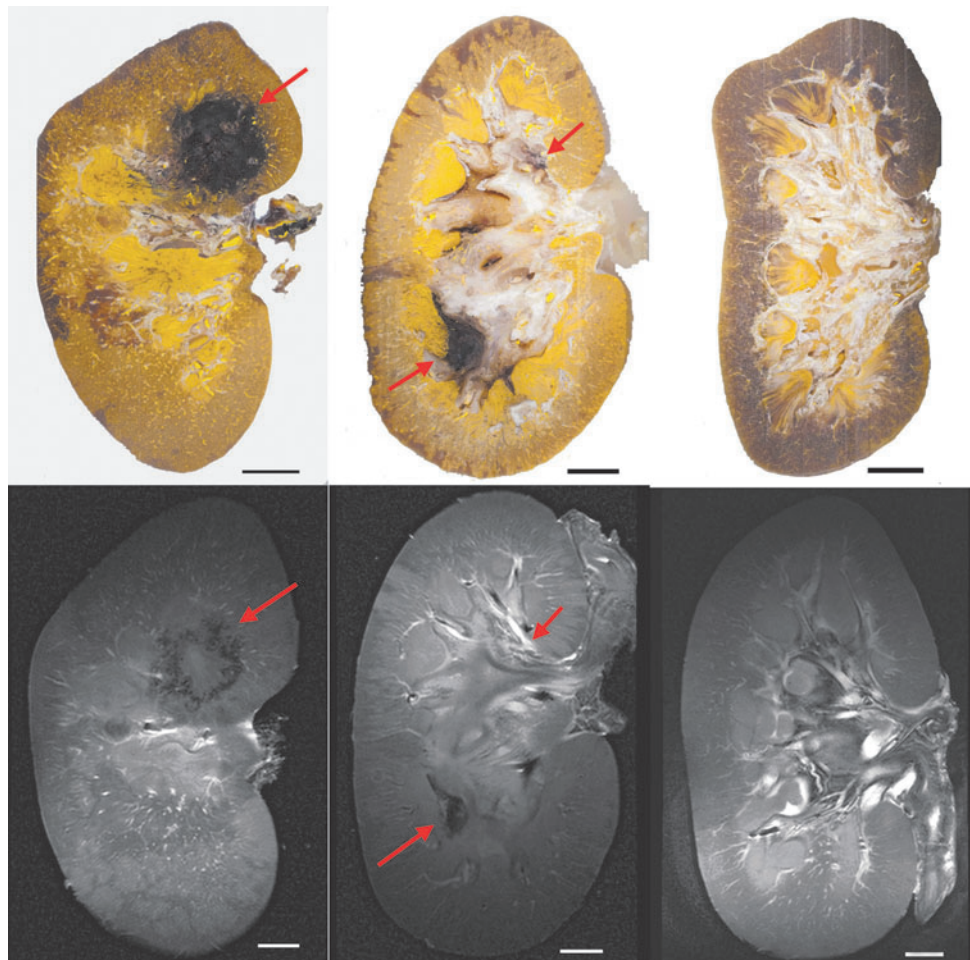


FIG. 2. Histomorphometric image slices (top row) and corresponding T2-weighted images (bottom row) with injury sites denoted by red arrows. Following the identification of treatment sites described in Fig. 3, left panels show injury site 2-M n; middle panels show injury sites 3-U and 3-L; and right panels show images from kidney 8, in which no hemorrhagic injury occurred. Scale bars represent 1 cm.

TABLE 1. INJURY VOLUME PER TREATMENT SITE

| Injury site ^a | Transducer frequency (kHz) | Total exposure (minutes) | US hyperecho duration (No. of BWL pulses/10 ³) | MRI injury volume (%) ^b | Morphometric injury volume (%) ^{b,c} | Focal pressure (MPa) ^d |
|--------------------------|----------------------------|--------------------------|--|------------------------------------|---|-----------------------------------|
| 1-M | 170 | 5.0 | 30.0 | 1.90 | 2.5 | 6.5 |
| 2-M | 170 | 17.0 | 37.0 | 2.40 | 5.2 | 6.5 |
| 3-U | 335 | 13.3 | 7.8 | 0.03 | <0.1 | 6.3–8.1 |
| 3-L | 335 | 14.0 | 2.6 | 0.07 | <0.1 | 7.3–8.1 |
| 4-U | 335 | 12.0 | 0.8 | 0 | <0.1 | 7.3–8.1 |
| 5-U | 335 | 15.1 | 2.0 | 0.03 | <0.1 | 6.6–8.1 |
| 6-U | 335 | 12.0 | 4.0 | 0.03 | <0.1 | 5.8–8.1 |
| 6-L | 335 | 8.3 | 11.0 | <0.01 | <0.1 | 6.6–8.1 |
| 7-U | 335 | 11.0 | 2.4 | 0.01 | <0.1 | 5.8–8.1 |
| 7-L | 335 | 10.7 | 0.8 | 0.07 | <0.1 | 6.6–8.1 |

^aClassified by kidney number in conjunction with U, M, or L to indicate upper pole, mid-pole, and lower-pole sites, respectively.

^bAll injury volumes reported as percent of functional renal volume, which excludes renal sinus structures.

^cThe minimum quantitative resolution of the histomorphometric technique is 0.1%.

^dBWL output pressure or pressure range where dynamic hyperechogenicity was observed on B mode US.

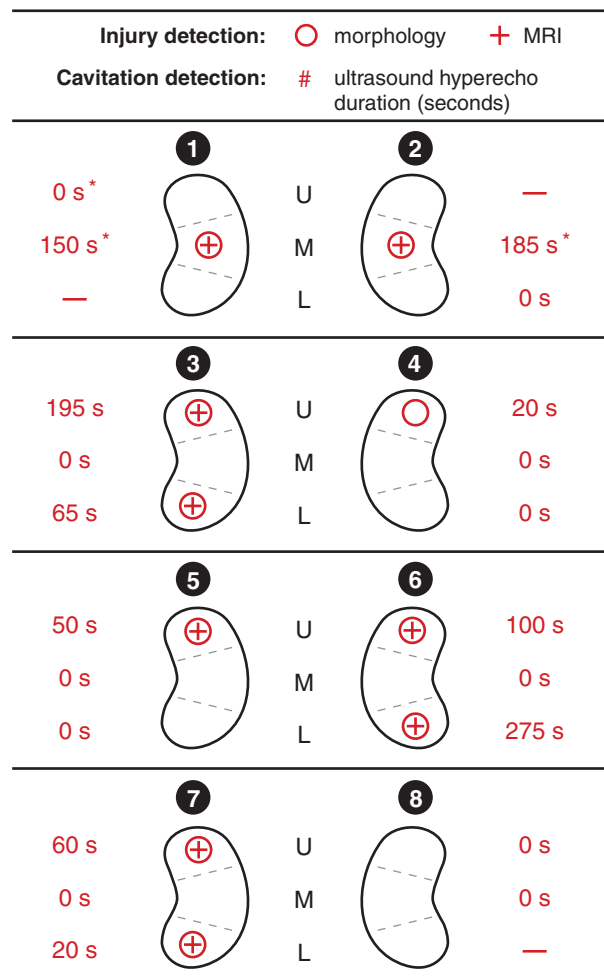
BWL = burst wave lithotripsy; US = ultrasound.

T1-weighted images (Fig. 1b), the relative intensity changes were variable. Susceptibility-weighted images appear to detect hemorrhage with the highest sensitivity, but overestimate the hemorrhagic volumes and lack anatomical detail.⁴ Figure 2 shows examples of the identification of large, small, and nonexistent injury in both histomorphometric and T2-weighted images.

BWL treatments were applied to 21 sites in 8 kidneys, with 3 sites serving as negative (untreated) controls. Exposure durations ranged from 5 to 21 minutes (Table 1 and Fig. 3). Of 21 sites treated with BWL, 10 (47.6%) had evidence of provoked hemorrhagic injury on histomorphometric analysis with the remaining 11 sites having no identifiable injury. Figure 3 shows the incidence and duration of cavitation on B-mode US and identification of injury on histomorphometric analysis and MRI. The sensitivity and specificity for US cavitation for identifying injury were both 100%. MRI was able to identify 9 of the 10 sites with hemorrhagic injury (sensitivity 90%) with no false positives (specificity 100%). Of the 11 sites where no injury was detected, exposure durations varied from 10 to 21 minutes, with focal pressure amplitudes from 6.5 to 8.1 MPa. These exposure parameters are within the range of those where cavitation and injury were observed (Table 1).

Volumetric quantification of injury by histomorphometric analysis and magnetic resonance imaging

Hemorrhagic injury sites and markers of renal anatomy were identified in 2D MRI image slices and integrated to estimate 3D volumes (Fig. 4). Table 1 shows comparison of the hemorrhagic injury volume as measured on histomorphometric analysis and T2-weighted MRI. For the eight sites treated at 335 kHz with identifiable injury, the lesion size determined by histomorphometric analysis was ≤0.1% of functional renal volume. On T2-weighted MRI, corresponding lesion volumes were also ≤0.1% of functional renal volume with a maximal detected injury of 0.07%. The remaining two lesions with larger measurable injuries were treated with the 170 kHz transducer (1-M, 2-M). Both techniques for injury quantification yielded lesion sizes 1.9% to



* Treatment bursts delivered at 200 Hz rate instead of 40 Hz.

FIG. 3. Detection of renal injury with morphometric and MRI. Each site is defined by a kidney number from 1 to 8 and “U,” “M,” or “L” to denote upper, mid, or lower pole, respectively. The duration of cavitation activity observed on B-mode US images is listed for each site (“—” indicates no BWL exposure). BWL = burst wave lithotripsy; US = ultrasound.

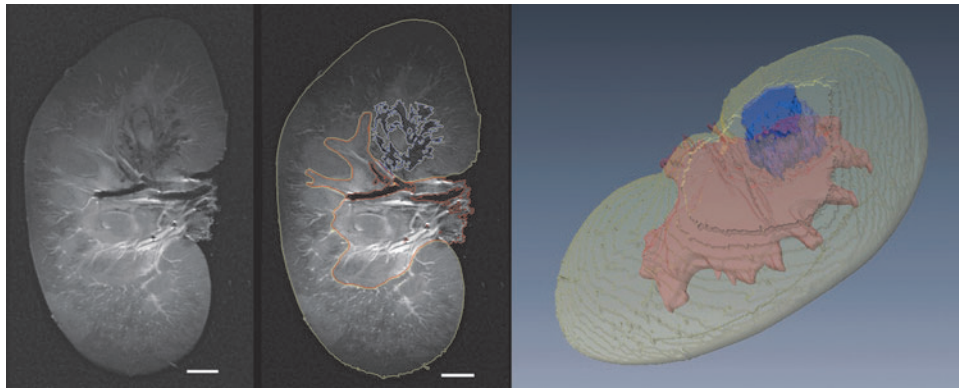


FIG. 4. Example of image segmentation to enable volumetric injury quantification of functional renal tissue. The two images at *left* show a raw T2-weighted image slice and the same image segmented to define areas representing functional tissue (yellow lines), renal sinus (red lines), and hemorrhagic injury in functional tissue (blue lines). A three-dimensional reconstruction of these volumes is presented at *right*. Scale bar represents 1 cm.

5.2% of functional renal volume, though the MRI estimates were 24% and 53% smaller.

Histologic characterization of renal lesions

Two kidneys were analyzed for histologic characterization of lesions. One site served as a negative control, two sites were treated at 170 kHz, and three sites were treated at 335 kHz. The injuries generated were histologically similar to those formed with SWL. Injury generated by both transducers showed evidence of intraparenchymal hemorrhage, with qualitative injuries including focal tubular injury/destruction and focal cellular fragmentation and necrosis (Fig. 5).

Discussion

BWL is an emerging technology for the treatment of renal stones; it has been demonstrated to fragment stones *in vitro* using relatively low-pressure bursts delivered at a fast rate. Because BWL uses US acoustic energy to break stones, there is potential to cause renal injury comparable to SWL.⁵ In SWL, quantifying renal injury is time consuming, technically challenging, and tissue destructive.² Accordingly, preclinical and clinical evaluation of BWL will be greatly aided by the

establishment of noninvasive, reproducible methods of injury detection and evaluation.

This study demonstrated that cavitation produced during BWL is observed as a region of dynamic hyperechogenicity on B-mode US.^{3,6-8} No injury occurred in this study without cavitation detected on US. This result suggests US should serve as a real-time method to monitor for cavitation to prevent renal injury during BWL treatment. If cavitation is detected the user could pause the treatment to allow the cavitation bubbles to clear before further treatment at the same or a reduced output level. This strategy will require prospective validation.

MRI evaluation of fixed *ex vivo* kidneys detected injury with a high degree of sensitivity and specificity. Only a single injured region seen on histomorphometric analysis was not initially seen on MRI (site 4-U). At this site, injury was missed on MRI because of the site's proximity to a renal cyst, but upon retrospective evaluation the hemorrhage was identified. Despite deliberate exposure of tissues to sustained cavitation during BWL treatment exposures, most of the acute hemorrhagic injury in this study was <0.1% functional renal volume on histomorphometric and MRI analyses. Although the small numbers do not allow a robust statistical comparison of lesion volumes for the two techniques, values

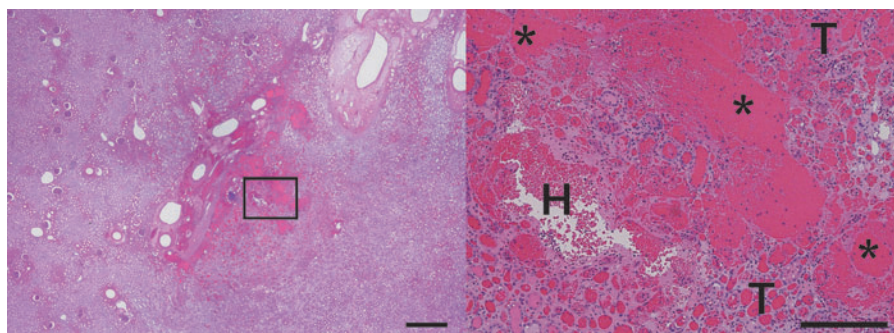


FIG. 5. H&E-stained sections showing an example of the typical histological injury produced with the 335 kHz BWL transducer. At low magnification (*left frame*, scale bar represents 1 cm), a small area of injury is observed within the parenchyma. At increased magnification (*right image*, scale bar represents 250 μ m) there is evidence of intraparenchymal bleeding (H), with qualitative injuries including focal tubular injury/destruction (T) and focal cellular fragmentation and necrosis (*). H&E, hematoxylin and eosin.

were similar with a relative underestimation of lesion size on MRI for the two largest lesions. This discrepancy may be due to differences in the determination of the renal sinus volume and functional renal volume, unequal dehydration and shrinkage of the injury lesion compared to the renal parenchyma, or fundamental differences in the detection of hemorrhage between the two techniques. Regardless, MRI detected even very low levels of acute hemorrhagic injury. In context, MRI is a natural alternative for rapid quantification of hemorrhage⁹ and is being actively investigated for quantifying hemorrhagic renal injury caused by SWL¹⁰ and for injury characterization and quantification in other mechanical US therapies, such as histotripsy.^{11,12}

The histologic pattern of renal injury for BWL was similar to what has been described in SWL-mediated injury.¹³ Hemorrhagic renal injury from SWL is hypothesized to be mediated through small vessel injury from cavitation.^{2,14,15} Shock waves can result in cavitation bubbles that grow and collapse with each pulse, causing mechanical trauma in their immediate vicinity.¹⁶ Similarly, our results are consistent with the interpretation that the amount of hemorrhagic injury was primarily determined by the number of affected vessels and the extent of injury for each. In particular, sizable injury was only detected for the two exposures at 170 kHz, for which the persistence and evolution of cavitation activity occurred over more BWL pulses (Table 1). Some lesions in our study show evidence of tissue homogenization, a characteristic of injury caused by certain shock wave lithotripters.^{17,18} Thermal injury with BWL is unlikely due to the low frequency and spatial-peak temporal-average intensity ($\leq 16.5 \text{ W/cm}^2$ in this study) in comparison to high-intensity focused US and similar technologies.¹

This study was not designed to assess BWL injury under clinical treatment parameters as we often allowed cavitation to persist to better characterize the injury. However, the focal pressure amplitude and total energy delivered in these experiments are comparable to those used to reliably fracture stones *in vitro*.¹ Even when cavitation was observed and the treatment was allowed to progress with cavitation, the volume of acute injury with the 335 kHz probe was $<0.1\%$ of functional renal volume. This level of injury represents the resolution of the histomorphometric technique and is unlikely to be clinically significant. BWL transducers with higher frequencies—335 kHz and above—have the additional benefit of producing smaller stone fragments during lithotripsy. Consequently, future efficacy and injury studies will primarily focus on transducers in the higher frequency range.^{1,19}

This study has several limitations. First, a limited sample size and variable treatment parameters were used. However, the presented data do demonstrate the utility of US imaging and MRI for identifying and assessing hemorrhagic injury induced by BWL. Histologic assessment of injury was only performed on a small subset of kidneys and treatment sites, though the histologic characteristics were consistent. Second, the implementation of BWL treatment delivery did not address physiological considerations relevant to injury: the treatment probe was placed directly on the kidney via laparotomy, and sequential exposures were delivered to multiple sites in each kidney, potentially affecting renal blood flow and injury progression.²⁰ However, with the exception of the two cases using the 170 kHz transducer, the volume of injury was uniformly small. For this reason

probe handling and treatment sequence had negligible impact on lesion size.

Despite these limitations, this study demonstrated that US can be used as a real-time method to monitor for injury during BWL. MRI also provided excellent sensitivity to detect even small areas of acute hemorrhagic injury and offers a viable alternative to histomorphometric analysis.

Conclusion

BWL is an emerging technology for the treatment of renal stones. Real-time US monitoring during BWL therapy allows detection of cavitation related to injury. This might allow the user to alter treatment to minimize or prevent renal injury. MRI also provides an alternative method to detect and quantify injury in a noninvasive manner. The combination of real-time assessment of cavitation on US and quantification of renal injury on MRI provides a framework for future preclinical testing of BWL.

Acknowledgments

We thank Rajash K. Handa, James A. McAteer, Bret A. Connors, and James C. Williams, Jr. for helpful discussions on renal injury evaluation and histology. We also acknowledge financial support from NIH through NIDDK P01 DK043881, K01 DK104854, R01-CA188654; from NSBRI through NASA NCC 9-58; and from resources through the VA Puget Sound Health Care System, Seattle, Washington.

Author Disclosure Statement

M.R.B., A.D.M., M.D.S., and B.W.C. have equity in and consulting agreements with SonoMotion, Inc., which has licensed technology related to this work from the University of Washington. The remaining authors have no competing financial interests.

References

1. Maxwell AD, Cunitz BW, Kreider W, Sapozhnikov OA, Hsi RS, Harper JD, et al. Fragmentation of urinary calculi *in vitro* by burst wave lithotripsy. *J Urol* 2015;193:338–344.
2. Blomgren PM, Connors BA, Lingeman JE, Willis LR, Evan AP. Quantitation of shock wave lithotripsy-induced lesion in small and large pig kidneys. *Anat Rec* 1997;249:341–348.
3. Hall TL, Fowlkes JB, Cain CA. A real-time measure of cavitation induced tissue disruption by ultrasound imaging backscatter reduction. *IEEE Trans Ultrason Ferroelectr Freq Control* 2007;54:569–575.
4. Schrag M, McAuley G, Pomakian J, Jiffry A, Tung S, Mueller C, et al. Correlation of hypointensities in susceptibility-weighted images to tissue histology in dementia patients with cerebral amyloid angiopathy: A postmortem MRI study. *Acta Neuropathol* 2010;119:291–302.
5. McAteer J, Evan A. The acute and long-term adverse effects of shock wave lithotripsy. *Semin Nephrol* 2008;28:200–213.
6. Li T, Khokhlova TD, Sapozhnikov OA, O'Donnell M, Hwang JH. A new active cavitation mapping technique for pulsed HIFU applications—Bubble Doppler. *IEEE Trans Ultrason Ferroelectr Freq Control* 2014;61:1698–1708.
7. Bailey MR, Pishchalnikov YA, Sapozhnikov OA, Cleveland RO, McAteer JA, Miller NA, et al. Cavitation detection during shock-wave lithotripsy. *Ultrasound Med Biol* 2005;31:1245–1256.
8. Vaezy S, Shi X, Martin RW, Chi E, Nelson PI, Bailey MR, et al. Real-time visualization of high-intensity focused

- ultrasound treatment using ultrasound imaging. *Ultrasound Med Biol* 2001;27:33–42.
9. Hammond NA, Lostumbo A, Adam SZ, Remer EM, Nikolaidis P, Yaghmai V, et al. Imaging of adrenal and renal hemorrhage. *Abdom Imaging* 2015;40:2747–2760.
 10. Handa RK, Territo PR, Blomgren PM, Persohn SA, Lin C, Johnson CD, et al. Development of a novel magnetic resonance imaging acquisition and analysis workflow for the quantification of shock wave lithotripsy-induced renal hemorrhagic injury. *Urolithiasis* 2017. [Epub ahead of print]; PMID: 28074231.
 11. Saeed M, Krug R, Do L, Hetts SW, Wilson MW. Renal ablation using magnetic resonance-guided high intensity focused ultrasound: Magnetic resonance imaging and histopathology assessment. *World J Radiol* 2016;8:298–307.
 12. Kim Y, Fifer CG, Gelehrter SK, Owens GE, Berman DR, Vlasisavljevich E, et al. Developmental impact and lesion maturation of histotripsy-mediated non-invasive tissue ablation in a fetal sheep model. *Ultrasound Med Biol* 2013;39:1047–1055.
 13. Shao Y, Connors B, Evan A, Willis L, Lifshitz D, Lingeman J. Morphological changes induced in the pig kidney by extracorporeal shock wave lithotripsy: Nephron injury. *Anat Rec A Discov Mol Cell Evol Biol* 2003;275:979–989.
 14. Matlaga BR, McAteer JA, Connors BA, Handa RK, Evan AP, Williams JC, et al. Potential for cavitation-mediated tissue damage in shockwave lithotripsy. *J Endourol* 2008; 22:121–126.
 15. Evan AP, Willis LR, Lingeman JE, McAteer JA. Renal trauma and the risk of long-term complications in shock wave lithotripsy. *Nephron* 1998;78:1–8.
 16. Zhong P, Zhou Y, Zhu S. Dynamics of bubble oscillation in constrained media and mechanisms of vessel rupture in SWL. *Ultrasound Med Biol* 2001;27:119–134.
 17. Parsons JE, Cain CA, Abrams GD, Fowlkes JB. Pulsed cavitation ultrasound therapy for controlled tissue homogenization. *Ultrasound Med Biol* 2006;32:115–129.
 18. Connors BA, McAteer JA, Evan AP, Blomgren PM, Handa RK, Johnson CD, et al. Evaluation of shock wave lithotripsy injury in the pig using a narrow focal zone lithotripter. *BJU Int* 2012;110:1376–1385.
 19. Maxwell A, Cunitz BW, Kreider W, Bailey MR, Sapozhnikov O, Lee FC, Sorensen MD, Harper JD. A preclinical image-guided therapy system for burst wave lithotripsy. *J Urol* 2015;193:e886.
 20. Willis L, Evan A, Connors B, Handa R, Blomgren P, Lingeman J. Prevention of lithotripsy-induced renal injury by pretreating kidneys with low-energy shock waves. *J Am Soc Nephrol* 2006;17:663–673.

Address correspondence to:
Mathew D. Sorensen, MD, MS

*Department of Urology
 University of Washington School of Medicine
 1959 NE Pacific Street
 Box 356510
 Seattle, WA 98195*

E-mail: mathews@uw.edu

Abbreviations Used

BWL = burst wave lithotripsy
 US = ultrasound
 MRI = magnetic resonance imaging
 SWL = extracorporeal shock wave lithotripsy
 H&E = hematoxylin and eosin